Supporting information

Effect of polymer concentration and cross-linking density on the microstructure and properties of polyimide aerogels

Ekaterina Filimonova[1,2], Thomas Bergmann[1], Shanyu Zhao[1], Valery A. Dyatlov[2], Wim J. Malfait[1*], Tingting Wu[1,3*]

[1] *Laboratory for Building Energy Materials and Components, Empa, Swiss Federal Laboratories for Materials Science and Technology, Überlandstrasse 129, 8600 Dübendorf, Switzerland.*

[2] *D. Mendeleev University of Chemical Technology of Russia, 9, Miusskaya Square, 125047, Moscow, Russia.*

[3] *Institute of Sustainability for Chemicals, Energy and Environment (ISCE[2]), Agency for Science, Technology and Research (A*STAR), 1 Pesek Road, Jurong Island 627833, Singapore.*

Email: wim.malfait@empa.ch, wu_tingting@isce2.a-star.edu.sg

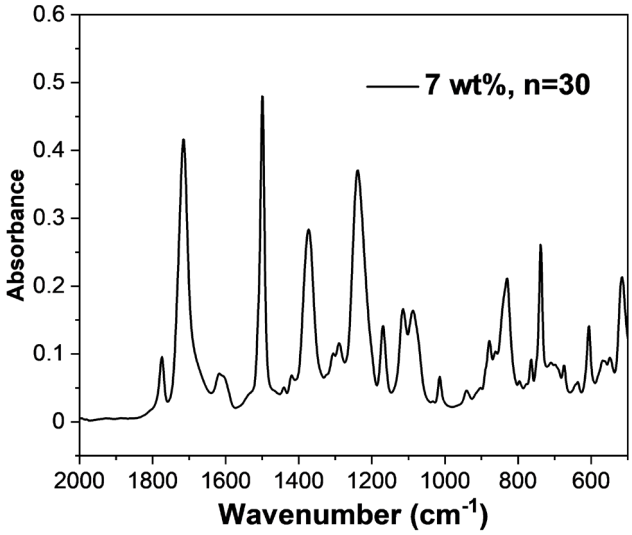

Figure S1. Fourier transform infrared (FTIR) spectrum of selected polyimide aerogel sample (7 wt%, 30n).

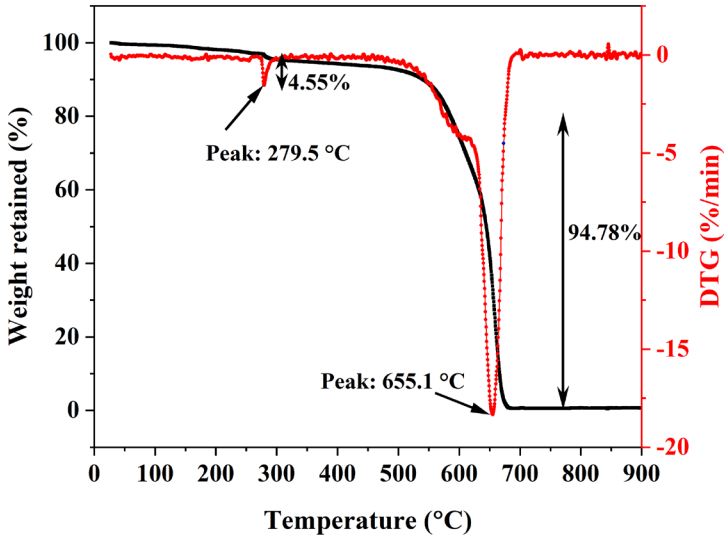

Figure S2. Thermogravimetry analysis (TGA) curve of selected polyimide aerogel sample (4 wt%, 45n).

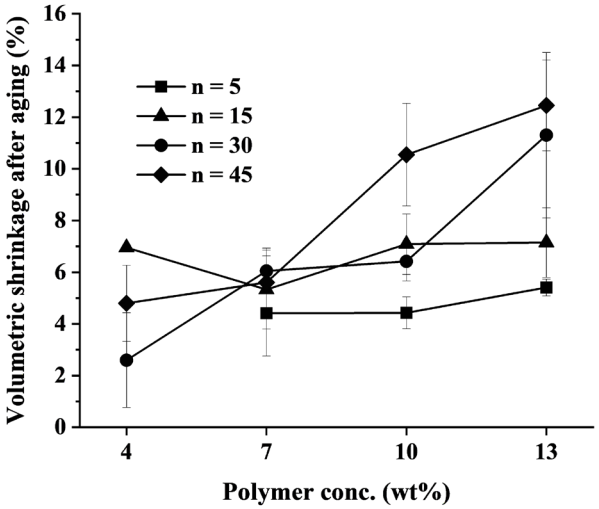

Figure S3. Volumetric shrinkage after aging *vs.* polymer concentration and number of repeat units n.

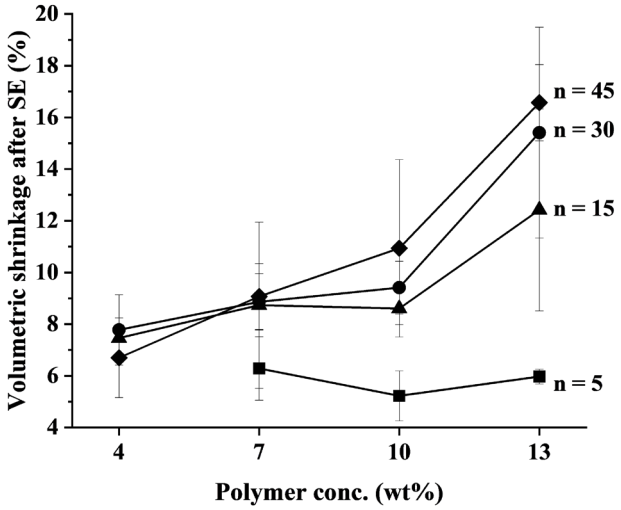

Figure S4. Volumetric shrinkage after solvent exchange (SE) *vs.* polymer concentration and number of repeat units n.

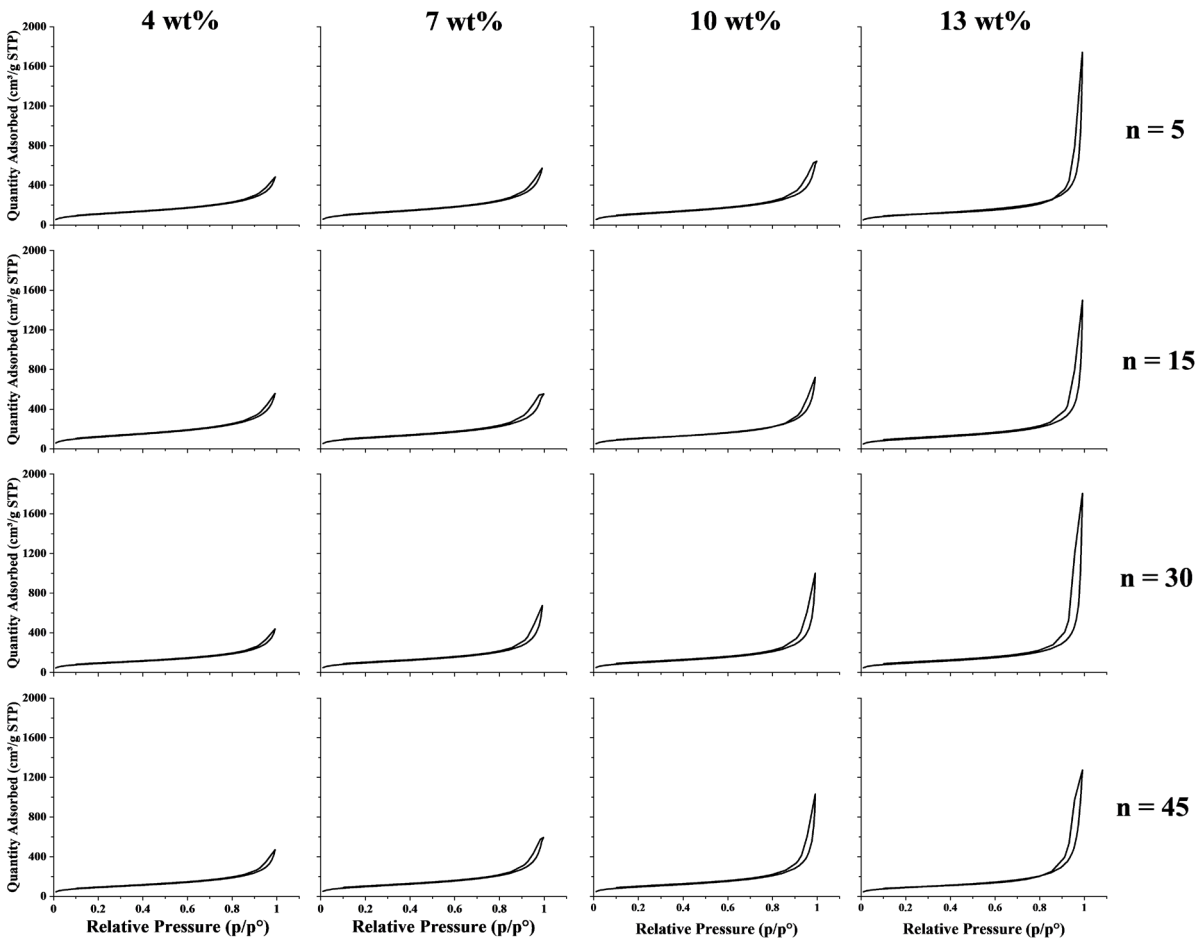

Figure S5. N_2 adsorption-desorption isotherms for all polyimide aerogels from this study.

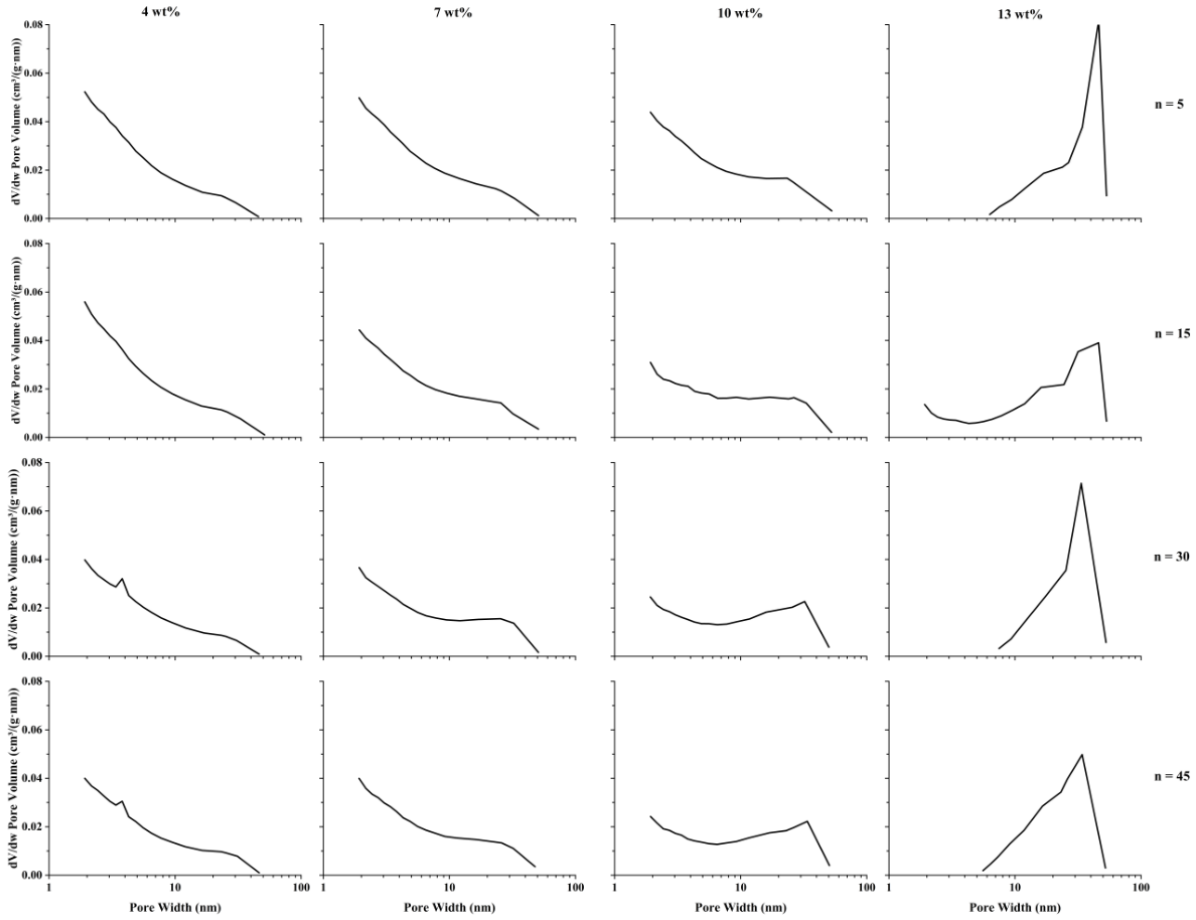

Figure S6. BJH pore size distribution for all polyimide aerogels from this study.

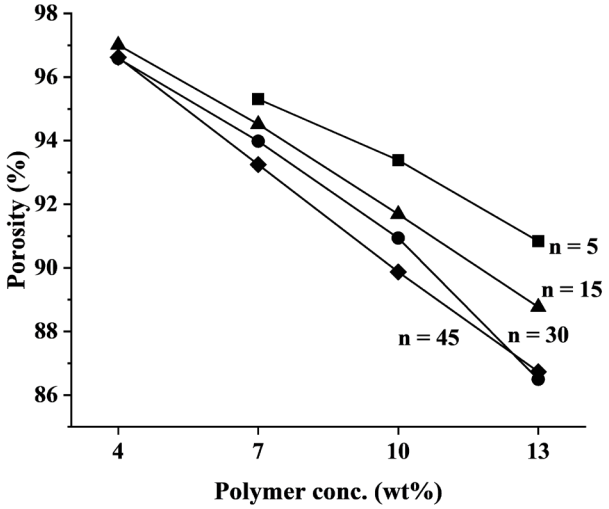

Figure S7. Porosity *vs.* polymer concentration and n.

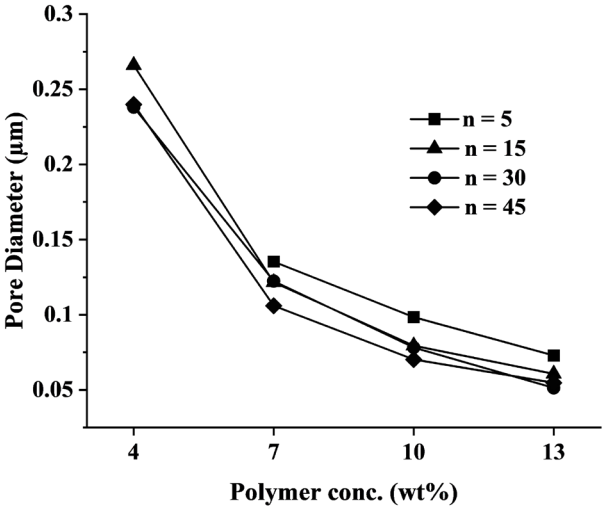

Figure S8. Pore diameter (calculated from density and surface area) *vs.* polymer concentration and number of repeat units n.

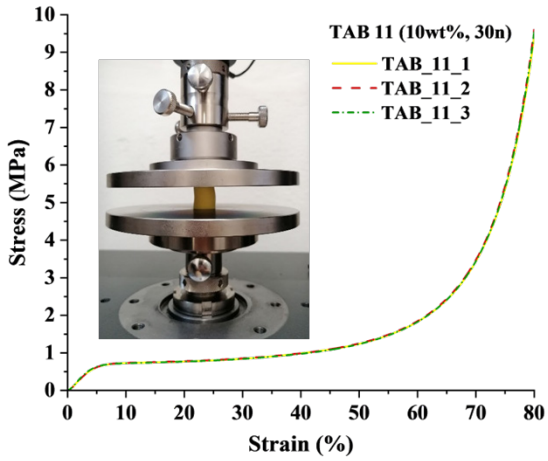

Figure S9. The three stress-strain curves from the same TAB 11 formulation show the repeatability of aerogel samples with the inserted compression testing photo.

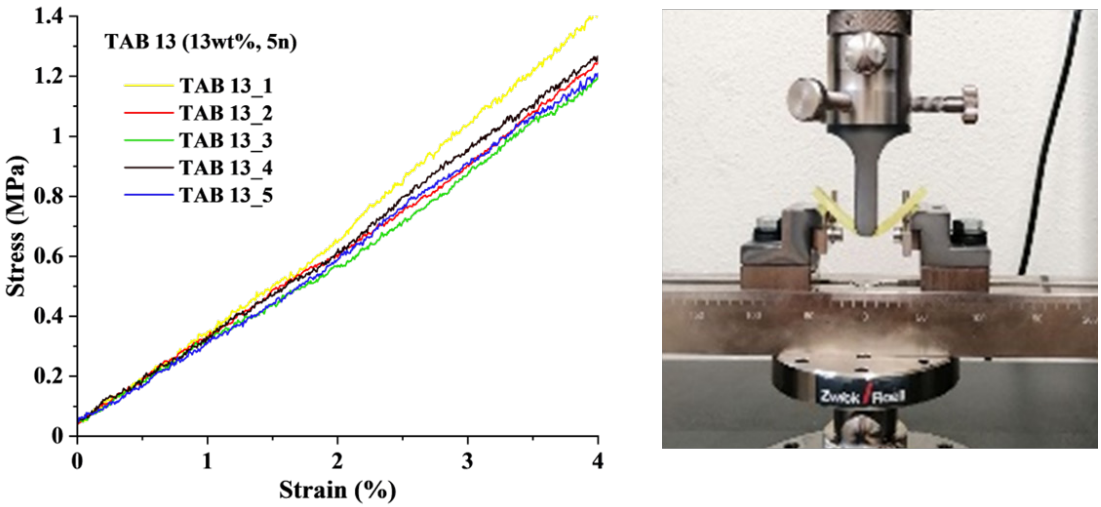

Figure S10. The 3-point bending stress-strain curves from the same TAB 13 formulation show the repeatability of aerogel samples. The picture of the 3-point bending setup mounted in a load frame specimen. The initial liner part of typical stress-strain curves from 3-point bending of selected series.

Table S1. The summary of density, shrinkage, porosity, and gelation time.

Samples	wt %	n	Average density (g cm^{-3})	Average shrinkage (%)			Porosity (%)	V pore cal. (cm^3g^{-1})	D pore cal. (nm)	Skeletal density (g cm^{-3})	Apparent gelation time (min)
				after aging	after SE	after SCD					
TAB 1	4	5				broken				1.491	150
TAB 2		15	0.045	7.0	7.5	18.6	97.0	21.8	266		140
TAB 3		30	0.051	2.6	7.8	26.5	96.6	19.0	238		115
TAB 4		45	0.050	4.8	6.7	23.6	96.6	19.2	240		116
TAB 5	7	5	0.070	4.4	6.3	16.9	95.3	13.6	135		45
TAB 6		15	0.082	5.3	8.7	27.5	94.5	11.6	122		44
TAB 7		30	0.090	6.1	8.9	30.5	94.0	10.5	122		40
TAB 8		45	0.101	5.6	9.1	37.7	93.3	9.3	106		38
TAB 9	10	5	0.099	4.4	5.2	20.1	93.4	9.5	98		13
TAB 10		15	0.124	7.1	8.6	31.8	91.7	7.4	79		10
TAB 11		30	0.135	6.4	9.4	38.5	90.9	6.7	78		9
TAB 12		45	0.151	10.6	10.9	44.2	89.9	6.0	70		10
TAB 13	13	5	0.137	5.4	6.0	28.1	90.8	6.7	73		7
TAB 14		15	0.167	7.2	12.4	39.9	88.8	5.3	61		5
TAB 15		30	0.201	11.3	15.4	50.4	86.5	4.3	51		4
TAB 16		45	0.198	12.5	16.6	51.3	86.7	4.4	55		2

Table S2. Specific surface area, mechanical properties, and thermal conductivity.

Samples	wt%	n	Surface area ($m^2 g^{-1}$)	Modulus (MPa)	Flexural modulus (MPa)	λ, ($mW\ m^{-1}K^{-1}$)
TAB 1	4	5	384	broken		
TAB 2		15	328	broken		26.3
TAB 3		30	319	1.72	4.49	25.7
TAB 4		45	320	1.77	4.11	25.2
TAB 5	7	5	403	3.92	broken	23.0
TAB 6		15	381	4.44	10.91	21.6
TAB 7		30	342	5.74	11.64	23.0
TAB 8		45	349	7.16	8.89	21.9
TAB 9	10	5	385	8.19	16.23	21.4
TAB 10		15	373	11.23	19.90	23.7
TAB 11		30	344	12.40	20.55	24.3
TAB 12		45	339	15.67	18.32	23.6
TAB 13	13	5	365	14.03	29.16	23.3
TAB 14		15	349	23.34	38.32	27.2
TAB 15		30	335	26.80	59.98	32.3
TAB 16		45	320	19.09	71.79	30.2